

Two, three and four photon absorption of naphthalene

J.C. Poveda, A. Guerrero, I. Álvarez, and C. Cisneros

*Laboratorio de Colisiones Atómicas Moleculares Instituto de Ciencias Físicas,
Universidad Nacional Autónoma de México,
Cuernavaca, Morelos, 62210 México,
e-mail: jkclimb@fis.unam.mx*

Recibido el 22 de mayo de 2009; aceptado el 9 de junio de 2009

The effects of the multiple-photon absorption on the ionization, MPI, and dissociation, MPD, of Naphthalene were investigated. Laser radiation of 266 nm at pulse widths of 4.5 ns and intensities of the order of 10^8 - 10^{10} W·cm⁻², and carrier gases, CGs, such as helium, neon, argon, krypton, and xenon were used. In order to identify the produced ions, the time of flight mass spectrometry technique, ToF-MS, was employed. From the experimental data the number of photons absorbed was calculated, being two at low energies per pulse, less than 1.0 mJ, where the parent ion, C₁₀H₈⁺, was detected, in agreement with the ionization energy of Naphthalene, 8.14 eV. Increasing the energy per pulse to more than 1.0 mJ, new ions were observed, and three and four photons processes were identified. The effect of the CG was also investigated: the ion yields change as a function of energy per pulse and the CG. A sequence of pathways for photoionization and photodissociation was proposed taking into account the energy per pulse, number of absorbed photons and normalized ion yields.

Keywords: Naphthalene; PAHs; MPI; MPD; ToF-MS.

Se investigó el efecto de la absorción múltiple de fotones en la ionización, MPI, y disociación, MPD, del Naftaleno. Para ello se utilizó radiación láser de 266 nm con anchos de pulso de 4.5 ns, e intensidades del orden de 10^8 - 10^{10} W·cm⁻², y diferentes gases acarreadores, CGs, como helio, neón, argón, criptón y xenón. La identificación de los iones resultantes de los procesos de MPI y MPD, se realizó mediante espectrometría de tiempo de vuelo, ToF-MS. De los datos experimentales se calculó el número de fotones absorbidos en los procesos mencionados, a bajas energías por pulso, menores que 1.0 mJ; se detectó principalmente el ión molecular, lo cual estuvo de acuerdo con el potencial de ionización del naftaleno, 8.14 eV. Al incrementar la energía por pulso, a más de 1.0 mJ, se observó la formación de nuevos iones, como una consecuencia de la absorción de tres y cuatro fotones. Se propuso una secuencia de rutas de fragmentación para los procesos MPI y MPD, teniendo en cuenta la energía por pulso, el número de fotones absorbidos y las eficiencias iónicas normalizadas. También se investigó el efecto de los CGs, y se observó que las eficiencias iónicas cambian al variar la energía por pulso y el CG.

Descriptores: Naftaleno; PAHs; MPI; MPD; ToF-MS.

PACS: 32.80.Rm; 33.80.-b; 33.80.Eh; 34.50.Gb

1. Introduction

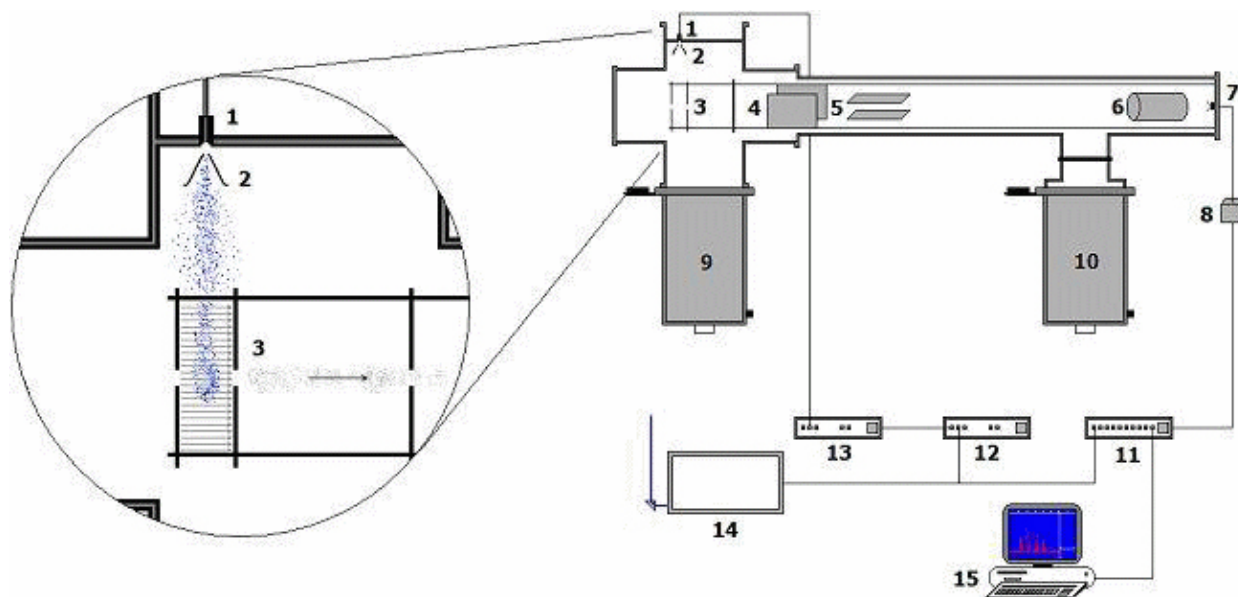
Laboratory studies in combination with theoretical quantum computations have provided a great deal of support in understanding the nature and relation of the PAH molecules with the interstellar emission observations. It is now clear that cationic forms of PAHs dominate these emissions [1-4]. In regions with higher UV photon densities, it is possible for the photo-destruction of PAHs to occur. On the other hand, the importance of PAHs [5-7] as carcinogenic substances and their presence in the environment as a result of combustion has been pointed out. These molecules can also be used as a model to understand some aspects of the interaction photon-molecule and related phenomena. However, in order to attempt a full understanding of the complicated multiphoton interaction processes more information is needed. In the present investigation Naphthalene, a PAH with atomic composition C₁₀H₈, is used as a model molecule to carry out experimental studies on photon-PAHs interactions.

In this paper the experimental results of the ionization and dissociation of Naphthalene will be discussed as a result of its interaction with laser pulse of 266 nm, 4.5 ns width, energies per pulse between 0.1 and 15 mJ, and repetition rate of 30 Hz,

with and without CGs as helium, neon, argon, krypton, and xenon. A ToF-MS technique was employed in order to identify the resulting photo-ions.

The structures of the polyatomic molecular systems determine the photo-physical properties and processes that can occur when they interact with photons in intense laser fields. Their ionization and dissociation are a result of the characteristics of laser radiation: photon energy, energies per pulse, and intensities, and also, the interaction of CGs with the molecule. In the nanosecond regimen, intensities of the order of 10^9 to 10^{12} W·cm⁻², ionization and dissociation are only possible by multiple-photon absorption as is shown in the present experiments.

DeWitt *et al.* [8] have reported the ionization and dissociation of PAHs and related hydrocarbons molecules, with 780 nm ultrashort laser pulses (170 fs) and intensities of up to 3.8×10^{13} W·cm⁻² in combination with ToF-MS and detected the formation of parent ions and multiple charged ions. Jochins *et al.* [9-11] had measured the photodestruction efficiency as a function of photon energy 5-25 eV using synchrotron radiation, and they observed the predominance of parent ions.



1. Pulsed valve, 2. Skimmer, 3. Extraction and acceleration plates, 4. and 5. Electrostatic lenses, 6. Einzel lens, 7. Detector, 8. Signal amplifier, 9. and 10. Vacuum system, 11. 12. and 13. Pulsed valve controller, delay system and data acquisition system, 14. Nd:YAG laser, 15. Personal computer

FIGURE 1. Experimental setup for MPI experiments.

TABLE I. Photophysical characteristics at 266 nm.

Property	value
t_{pulse} , ns	4.5
E_{pulse} , mJ	0.1 – 20.0
I , $W \cdot cm^{-2} / 10^9$	0.05-9.24
$\phi \times 10^{-24}$, photons $\cdot s^{-1}$	2.38
$\phi \times 10^{-16}$, photons-per pulse	1.07
Effective I.P., eV	8.140
Required n for PI	2
ϕ photon flux	

In the present work the molecular parent ion was mainly detected at low energies per pulse, where the two-photon absorption occurs by a resonant mechanism, (1+1) through the S_2 state.

As the energy per pulse was increased, the resulting photoions were identified and the possibility of more than two photon absorption from the neutral molecule is discussed, according to the previous reports on the electronic structure of Naphthalene. The number of photons absorbed to ionize or dissociate the molecule has been calculated for each ion group, showing that these processes occur as a consequence of multiple photon absorption. Also the effect of different inert CGs such as helium, neon, argon, krypton, and xenon

on the MPI was analyzed in terms of the number of absorbed photons. From these data sequential dissociation pathways were proposed considering the relation between precursors and daughter ions, as a function of energies per pulse, number of absorbed photons, and normalized ions yields.

2. Experiment

Figure 1 shows the experimental setup which has been described in Ref. 12. The Naphthalene sample was located in a thermal reservoir with a controller; the vapor pressure was increased by raising the temperature up to 373 K. The sample vapor was introduced into the ionization region using a pulsed valve synchronously coupled to the laser pulse. The molecular jet was generated by adiabatic expansion using a skimmer in a high vacuum region at 2×10^{-8} torr. Two conditions were considered in producing the molecular jet; first, no CG was used, only differential pressure makes it possible to introduce the sample. Secondly, mentioned CGs at pressures up to 40 psi in the thermal reservoir, were used. The final pressure in the ionization chamber reaches 2×10^{-6} torr. The neutral molecules interact orthogonally with the laser radiation of 266 nm, from the fourth harmonic of Nd: YAG laser, with 4.5 ns pulse width, and a repetition rate of 30 Hz. The laser radiation was focused into the interaction region using a lens with a focal length of 25 cm. The ToF spectra were taken at 50 different energies per pulse energy in the interval from 0.1 to 15 mJ, up to $2.5 \times 10^{10} W \cdot cm^{-2}$ equivalent intensities.

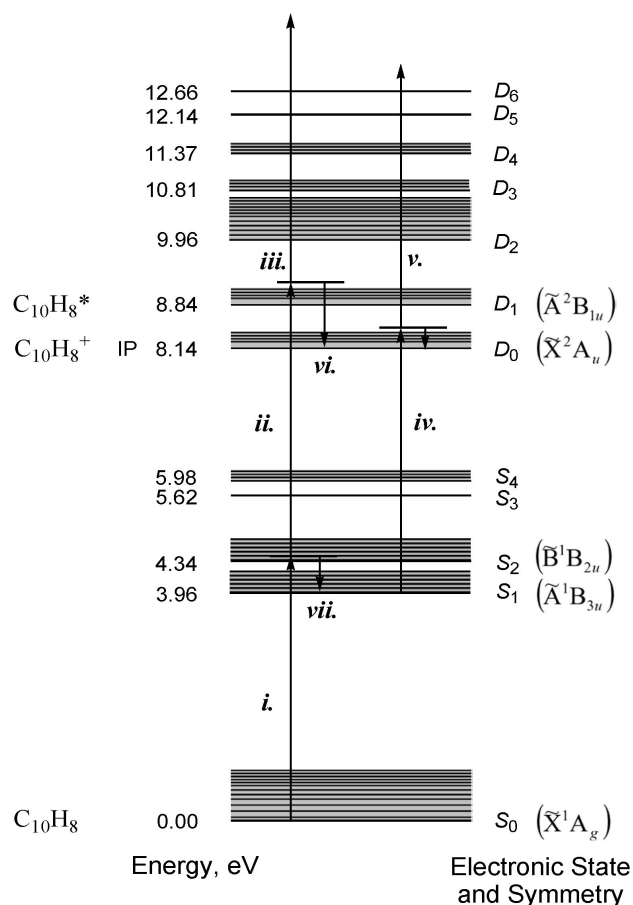


FIGURE 2. Electronic states and energies of Naphthalene.

The ions resulting from MPI and MPD were extracted from the interaction region by a 5.0 keV plate, and leaving with a final energy of 3.5 keV after a second parallel plate. They entered a drift region (field free), one meter long, and recorded using a channel electron multiplier detector. The signal from the detector was pre-amplified and digitized using a multichannel analyzer Turbo MCS EG&G Ortec. 5000 laser shots were collected and added, at each energy per pulse. A ToF window from 0 to 20 μ s, with 4000 channels, 5 ns per channel, was used to obtain the final ToF spectrum.

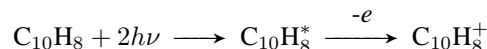
3. Results and Discussion

Within the present experimental conditions multiple photon absorption takes place. The photo-physical properties of Naphthalene and characteristics of the radiation pertained to this work are presented in Table I.

The first three electronic transitions of Naphthalene are observed in the near-UV region [13,14]. The first is a $S_1 \leftarrow S_0$ to excited singlet state of B_{2u} symmetry, with energy at 3.96 eV and oscillator strength 0.002. The $S_2 \leftarrow S_0$ transition has been reported [15] as a transition to a state with symmetry 2^1B_{1u} , energy of 4.34 eV, oscillator strength 0.18. The strongest $S_3 \leftarrow S_0$ transition to a B_{3u} state has energy of 5.62 eV and oscillator strength of 1.3 [16]. Some of the

energy levels and vibrational frequencies of the Naphthalene have been collected from the available literature [14,15,17] and are shown in Fig. 2. Bearing that in mind we interpreted the experimental results as follows:

At 266 nm a photon with an energy of 4.66 eV can be resonantly absorbed [18] to a vibrational level of the second excited state, S_2 ; with a second photon the molecule reaches the energy of a superexcited state which decays, leaving an ionized molecule and one free electron:



In Fig. 3 the ToF spectra at different energies per pulse at 266 are shown; as has been pointed out, at low energies per pulse only the parent ion was observed. As the intensity increases, new lighter ions appear as a result of the increase in the number of absorbed photons, which opens new dissociative channels.

In order to estimate the number of photons absorbed to form a particular ion, the logarithm of the measured photoion current was plotted as a function of the logarithm of the laser intensity according to the following relation:

$$C = f(\sigma_n) \cdot I^n \quad (1)$$

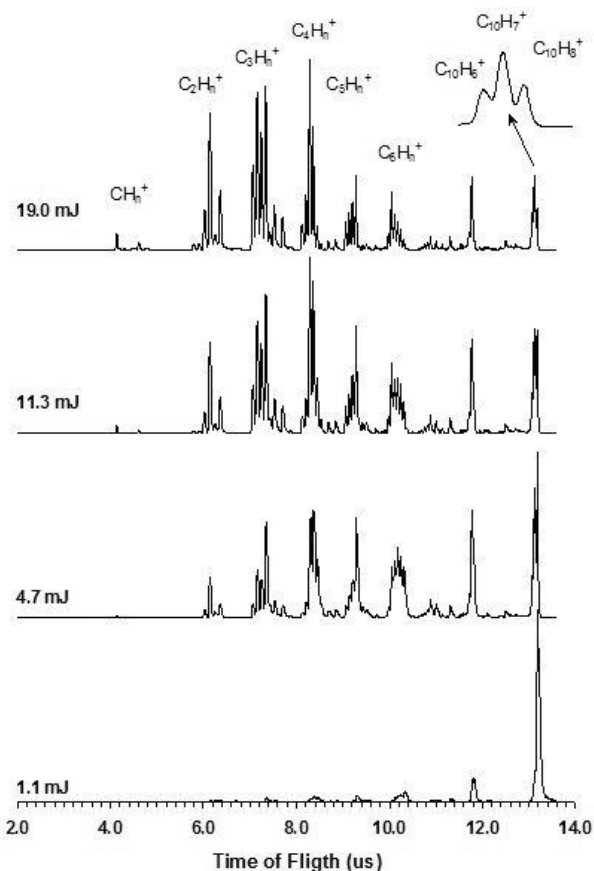


FIGURE 3. MPI-ToF spectra of Naphthalene at 266 nm.

TABLE II. MPI of Naphthalene at 266 nm. Number of absorbed photons.

Ion	NCG	Carrier Gas				
		He	Ne	Ar	Kr	Xe
CH_n^+	1.99 ± 0.10	3.26 ± 0.16	3.99 ± 0.20	3.84 ± 0.19	4.02 ± 0.20	4.09 ± 0.20
C_2H_n^+	2.88 ± 0.14	3.57 ± 0.18	3.33 ± 0.17	3.18 ± 0.16	3.03 ± 0.15	3.78 ± 0.19
C_3H_n^+	3.38 ± 0.17	3.07 ± 0.15	3.99 ± 0.20	2.01*	3.39 ± 0.17	2.89 ± 0.14
C_4H_n^+	3.85 ± 0.19	3.26 ± 0.16	3.80 ± 0.19	3.49 ± 0.17	3.81 ± 0.19	3.88 ± 0.19
C_5H_n^+	3.06 ± 0.15	3.21 ± 0.16	3.17 ± 0.16	3.12 ± 0.16	2.96 ± 0.15	3.00 ± 0.15
C_6H_n^+	2.82 ± 0.14	3.25 ± 0.16	2.95 ± 0.15	2.85 ± 0.14	3.04*	2.93 ± 0.15
C_7H_n^+	2.86 ± 0.14	3.03 ± 0.15	2.94 ± 0.15	2.43 ± 0.12	1.47*	3.00 ± 0.15
C_8H_n^+	2.14 ± 0.11	2.99 ± 0.15	3.00 ± 0.15	2.99 ± 0.15	2.70 ± 0.14	2.92 ± 0.15
C_9H_n^+	2.09 ± 0.10	3.03 ± 0.15	2.63 ± 0.13	2.95 ± 0.15	3.02 ± 0.15	2.69 ± 0.13
$\text{C}_{10}\text{H}_6^+$	2.45 ± 0.12	3.23 ± 0.16	3.20 ± 0.16	3.09 ± 0.15	3.30 ± 0.17	3.35*
$\text{C}_{10}\text{H}_7^+$	2.17 ± 0.11	3.02 ± 0.15	2.91 ± 0.14	2.67 ± 0.13	2.55 ± 0.13	2.54*
$\text{C}_{10}\text{H}_8^+$	2.07 ± 0.10	1.83 ± 0.09	2.01 ± 0.10	1.82 ± 0.09	1.74 ± 0.09	1.53*

* Overlapped with carrier gas ions.

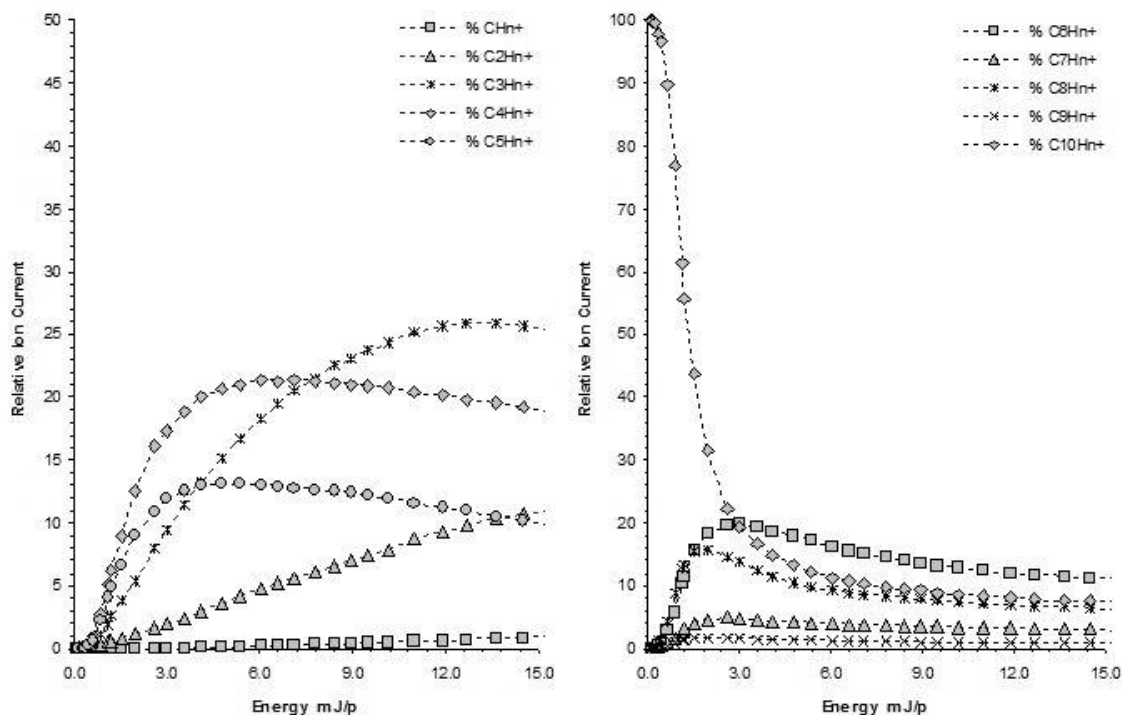


FIGURE 4. Relative IC as a function of energy per pulse. Neon as CG.

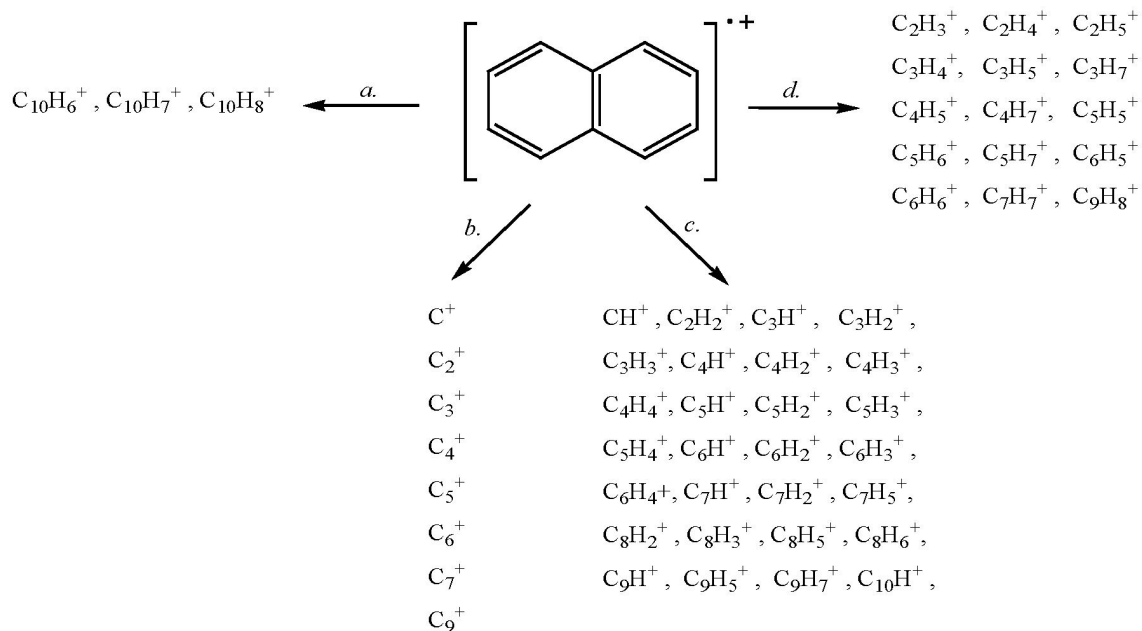
where C is the photoion current, $f(\sigma_n)$ is a function of the cross section for a particular process, and n is the order of the process or number of photons required to ionize the molecule or open a new dissociative channel.

Ions were grouped according to the number of carbon atoms, C_nH_m^+ , n from 1 to 10. In Fig. 4 relative ion currents for the formation of each observed ion group, as a function of energy per pulse, are shown. From those ion currents the

number of photons was calculated with and without CGs, and the results are shown in Table II.

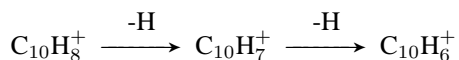
3.1. Ion products

The detected ions have been classified according to the possible dissociation channels, and different mechanisms are proposed to interpret some of our observations. The resulting ions from the MPI and MPD of Naphthalene are displayed in the following diagram:

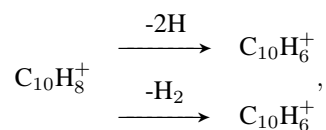


Hydrogen loss:^a

At 266 nm laser radiation, molecular ion and its deprotonated ions were observed as the pulse laser intensity was increased. $C_{10}H_8^+$, $C_{10}H_7^+$ and $C_{10}H_6^+$ were detected as shown in Fig. 3. Va-Oanh [19] proposed two different deprotonation pathways for the case of fluorene which can be extended for Naphthalene: a sequential and a concerted dissociative process. In the former case, two neutral hydrogen atoms are lost in a step by step process:



in the latter, two neutral hydrogen atoms or molecular hydrogen are simultaneously eliminated:



Jobilois [20] had calculated the energy for the sequential and concerted double hydrogen loss mechanism, being of the order of 10.31 eV and 5.76 eV, respectively. In the present

TABLE III. Energy[&] at Maximum Ion Yield in the MPI experiments of Naphthalene.

Ion	WCG	Carrier Gas				
		Helium	Neon	Argon	Krypton	Xenon
$C_2H_n^+$	6.05	5.99	9.10	7.71	11.03	13.99
$C_3H_n^+$	5.94	5.21	6.35	5.65	8.71	12.03
$C_4H_n^+$	4.37	3.43	3.89	5.68	4.99	9.86
$C_5H_n^+$	3.58	2.95	3.57	4.33	5.09	7.88
$C_6H_n^+$	2.61	2.17	2.73	3.34	4.65	6.63
$C_7H_n^+$	2.32	2.12	2.64	4.44	3.64	6.31
$C_8H_n^+$	1.75	1.87	2.27	2.92	3.19	4.78
$C_9H_n^+$	2.18	1.90	2.32	3.86	3.63	4.85
$C_{10}H_n^+$	0.50	0.38	0.24	1.03	1.05	1.66

[&]Values in mJ per pulse

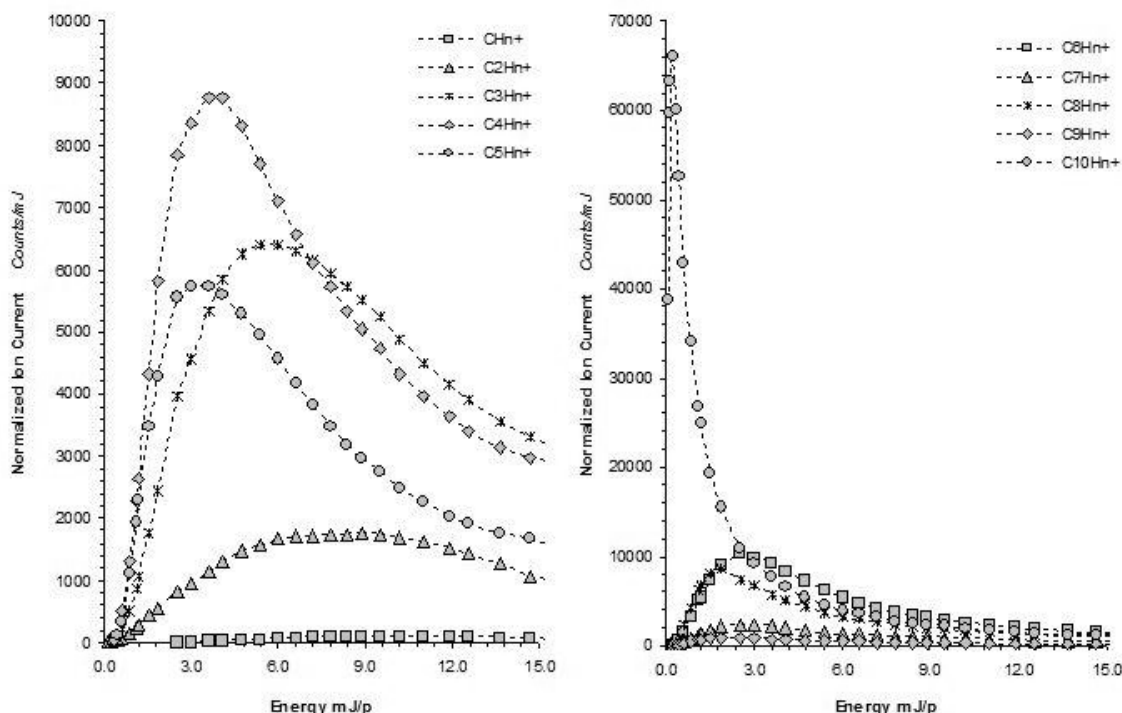


FIGURE 5. Normalized IC as a function of energy per pulse. Neon as CG.

experiment, both cases were observed. At energies per pulse of less than 7 mJ, the total parent ion current decreases as a consequence of the sequential mechanisms, $C_{10}H_7^+$ and $C_{10}H_6^+$ ion currents increase monotonically as a function of energy per pulse. At energies greater than 7 mJ, the $C_{10}H_7^+$ ion current reaches a plateau, while the ion currents of $C_{10}H_8^+$ and $C_{10}H_6^+$ decreases and increases, respectively; this fact can be explained as the loss of H_2 and the formation of $C_{10}H_6^+$. Ho [20] measured the C-H bond dissociation per proton of $C_{10}H_8^+$ and found it is of the order of 4.48 eV, while Reed [22] reported dissociation energies of 4.86 eV. In our experiments, deprotonation of $C_{10}H_8^+$ was the result of the absorption of an additional photon of energy of 4.66 eV, since H^+ , and H_2^+ were not detected; it is possible then that the hydrogen loss takes place through neutral hydrogen elimination. Measurements were also taken for the formation of $C_{10}H_8^+$, $C_{10}H_7^+$ and $C_{10}H_6^+$ as a function of the CG, and it was observed that the heavier CG acts in favor of deprotonation of $C_{10}H_8$.

Total deprotonation and formation of carbon clusters: b

The formation and detection of carbon clusters C_n^+ , $n=2$ to 9, from PAH such as Naphthalene is evidence of the structural stability of electronic resonant rings in PAHs. In our experiments, carbon clusters from two to nine carbon atoms were detected; that may suggest that the cluster formation does not occur by a simultaneous dissociative process. The carbon clusters ions are the result of a sequential dissociation.

Molecular fragmentation without hydrogen transposition: c

This ion group constitutes the most abundant type of ions observed in the PD of Naphthalene, but they are not responsible for the high ion currents. They may be the result of a simple dissociation of molecular ion or the daughter ions.

Intramolecular hydrogen transposition and formation of highly protonated ions: d

Several of the ions identified have a H/C ratio higher than one. This fact is possible because hydrogen transposition can occur when the molecular ions or daughter ions are dissociated. Some examples of such ions are $C_2H_n^+$, $C_3H_n^+$ and $C_4H_n^+$ series with n higher than 2, 3, and 4, respectively.

3.2. Sequence photon absorption-dissociation, connecting daughter to parent ions, pathways

In this section the sequence of photon absorption-dissociation is analyzed. In order to estimate the maximum ion current as a function of the energy per pulse, each particular ion group, was normalized relative to the energy per pulse; the results are shown in Fig 5. Such maxima are an indication of the energy where the processes are more efficient. In Table III the maxima are reported for each case, with and without CG. These results, together with calculated number of absorbed photons, Table II, have been used to propose sequential dissociation pathways of Naphthalene. As can be seen, there

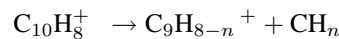
is a sequence of maxima displaced to higher energies corresponding to lighter ions. A decrease in the normalized ion current for a particular ion indicates the opening of a new dissociative channel. From this behavior it is possible to establish a relationship between parent and daughter ions. The following discussion is based on the data obtained when Ne was used as CG; similar reasoning can be extended to all the cases studied.

At low energies per pulse, less than 0.24 mJ/p, Fig. 3, mainly the parent ion is observed, two-photon absorption, 9.32 eV. The energy of the two photons is enough for the electron to reach the continuum with an excess of 1.22 eV; steps *i* and *ii* or the molecular ion reach the D_1 electronic excited, Fig. 2. If $C_{10}H_8^+$ ion is in the D_1 state, it is possible for it to absorb additional photons, step *iii* in Fig. 2, or decay to the D_0 state by a vibrational relaxation, step *vi* in Fig. 2.

As the energy per pulse increases, the absorption of more than two photons to higher excited states that can lead to fast ionization-dissociation processes. If this is the case all ions will have the maximum yield at the same energy per pulse. However, our results showed different values for these maxima (Table III). Different maximum values for the energy per pulse may indicate that, even if the number of photons is the same, one specie can be the precursor of the next one, as will be discussed below.

With the absorption of two photons, the molecule may reach an ionized state with an energy excess, D_1 excited electronic state, and with an additional photon, the ion can be promoted to D_n electronic state with $n > 6$, which in turn dissociates, producing the daughter ions: $C_6H_{8-n}^+$, $C_7H_{8-n}^+$, $C_8H_{8-n}^+$, and $C_9H_{8-n}^+$. According to the results from Table II, almost the same number of photons are needed for them to appear and their energy per pulse maxima are very close, Table III.

The $C_9H_{8-n}^+$ and CH_n^+ ion currents are very low; these are non favorable energy processes and may be the result of:



or



The formation of $C_8H_{8-n}^+$ can be explained by the acetylene lost from the molecular ion as: $C_{10}H_8^+ \rightarrow C_8H_{8-n}^+ + C_2H_n$, and its contribution reaches a maximum of 16% from the total ion current, at 2.27 mJ per pulse, step *ii* in Fig. 6.

The $C_7H_{8-n}^+$ results from the dissociation of the molecular parent ion as follows: $C_{10}H_8^+ \rightarrow C_7H_{8-n}^+ + C_3H_n$. $C_3H_n^+$ has been detected at higher energies per pulse, and then it is produced by a different dissociation channel, as will be explained. This is a non-favored process: the ion yield reaches only 4 % at 2.94 mJ per pulse, step *i* in Fig. 6.

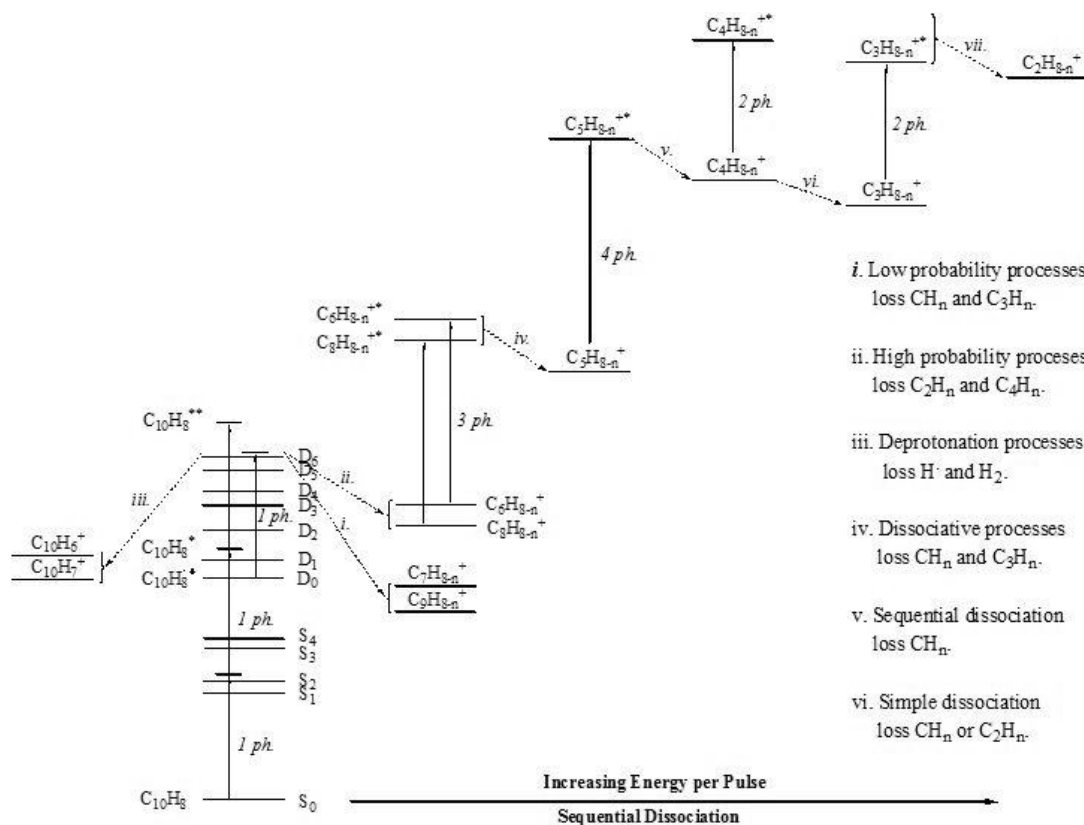


FIGURE 6. Dissociation pathways in MPI of Naphthalene at 266 nm. Neon as CG.

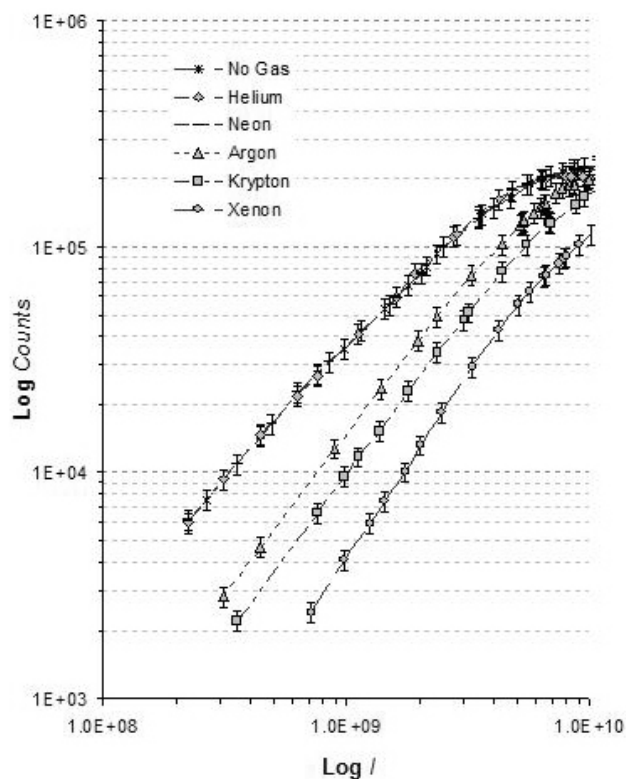


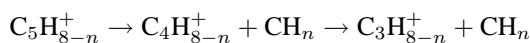
FIGURE 7. Log-Log plot of TICs with different CG.

The formation of $C_6H_{8-n}^+$ can be explained as the result of two different processes: first, a direct dissociation of $C_{10}H_8^+$ as follows: $C_{10}H_8^+ \rightarrow C_6H_{8-n}^+ + C_4H_n$; second, $C_6H_{8-n}^+$ could come from the loss of two acetylene fragments one from $C_{10}H_{8-n}$ as follows: $C_{10}H_8^+ \rightarrow C_8H_6^+ + C_2H_2 \rightarrow C_6H_4^+ + C_2H_2$. The formation of $C_6H_{8-n}^+$ is a process with relatively high probability, being 21 % of the total ion current at 2.73 mJ per pulse, step *ii* Fig. 6.

$C_5H_n^+$ ion formation reaches its maximum at 3.57 mJ per pulse; its formation is interpreted as being the result of the dissociation of $C_8H_n^+$ and $C_6H_n^+$, in high the vibrational states, step *iv*. Figure 6:



The number of photons calculated to form $C_4H_n^+$ and $C_3H_n^+$ are almost the same, of the order of four; nevertheless, their maxima appear at two different values of energy per pulse 3.89 and 6.35 mJ, respectively, Table II, steps *v* and *vi* Fig. 6. Their formation can be explained by a sequential dissociation:



$C_2H_n^+$ is a product of different dissociative processes, with its maximum at 9.10 mJ per pulse.

The present results are in very good agreement with previous measurements with regard to the energies needed to form different species, as reported by Gotkins [23] and Jochins [24]. Jochins classified the unimolecular decomposition of Naphthalene ion in two groups: low-energy and high-energy; the first case up to 15 eV, where the ring structure is preserved, corresponds to three-photon processes in the present work, and accounts for the formation of ions from $C_9H_{8-n}^+$ to $C_5H_{8-n}^+$. The second regime involves processes which require more than 15 eV, and the opening of the ring structure; these correspond to the four-photon processes reported here.

3.3. Carrier gas effect

In this section, a brief interpretation is given of the experimental results when inert CGs are used to improve the transport of Naphthalene vapors. The sample was combined with helium, neon, argon, krypton, and xenon individually, at a final pressure up to 40 psi. The influence of the CG was observed in two different scenarios: the number of absorbed photons required to open a specific dissociative channel, Table II, and the total ion current, Fig. 7. In the first case, within experimental error, the number of photons to induce the dissociation process is very close; changes in the energy to induce particular processes were not observed. Evidence of the formation of van der Waals complexes, *Naphthalene-CG*, was not shown in the analysis of detected ions. However, it was observed that, as the mass of the CG increases, the total ion current decreases and its maximum is shifted to higher energies per pulse, Fig. 7.

Also, it is worth mentioning that ions of CGs were detected under the present conditions. When argon was used as CG, isotopic composition 36 (0.336 %), 38 (0.063 %), and 40 (99.600 %), there is an overlap of the corresponding ions with $C_3H_n^+$ ions, with n equal to 0, 2 and 4. A similar situation was observed with krypton as CG, which has an isotopic composition of 78 (0.35 %), 80 (2.28 %), 82 (11.58 %), 83 (11.49 %), 84 (57.00 %) and 86 (17.30 %). The ions were separated into two groups: the first overlaps with signals from $C_6H_6^+$ (78) and $C_6H_8^+$ (80) ions; the second, with C_7^+ (84) and $C_7H_2^+$ (86) ions.

The fact that the total ion current diminishes as the mass of the CG increases can be interpreted as a change in the ratio of Naphthalene to CG quantities in the interaction region. As the mass of gas increases, the mean velocity decreases; for lighter atoms such velocities are higher than the mean velocity attained by the Naphthalene molecules, becoming very similar when Xe was used, as shown in Fig 7.

4. Conclusions

The MPI of Naphthalene has been studied using a ToF-MS technique combining a laser along with a molecular jet, in order to investigate the effects of the wavelength, intensity and CG on the different mechanisms that lead to the wide variety

of ion products. An attempt to interpret the rich and complex spectra has been made, proposing different dissociation pathways. With low intensity 266 nm laser radiation, a MPI-MPD process is induced by resonant two-photon absorption. An increase in the total ion currents was observed as the intensity increases, and new ions were produced as result of the opening of new dissociative channels, until Naphthalene was completely photodissociated. Sequential loss of acetylene leading to the dissociation of Naphthalene cation has been observed by Ekern [25], and the present results agree with his observations. From the analysis of the ion currents of individually ion groups [Eq. (1)] the number of absorbed photons was cal-

culated. The ion currents were normalized, and together with the calculated number of photons were combined in order to relate a particular photon absorption-dissociation channel to the resulting parent-daughter ions and propose an ionization-dissociation scheme. The effect of CG cannot be neglected: the total and partial ion currents change as a function of them.

Acknowledgements

The authors wish to express their thanks for the financial support of DGAPA-PAPIIT grants IN-109407, IN-10809, and CONACYT grants 24929 and 82521.

1. L.J. Allamandola, A.G. Tielens, and J.R. Barker, *Astrophys. J. Supp. Ser.* **71** (1989) 733.
2. G.H. Herbig, *Annu. Rev. Astrophys.* **33** (1995) 19.
3. T.W. Smith and R.G. Sharp, *Aust. J. Chem.* **58** (2005) 69.
4. G. Mula, G. Mallocci, and I. Porceddu, *J. Phys.: Conf. Ser.* **6** (2005) 217.
5. D. Rolland, A.A. Specht, M.W. Blades, and J.W. Hepburn, *Chem. Phys. Lett.* **373** (2003) 292.
6. R.S. Braga, P.M.V.B. Barone, and D.S. Galvao *Journal of Molecular Structure: THEOCHEM* **464** (1999) 257.
7. T. Pino, P. Parneix, F. Calvo, and Ph. Bréchnignac, *J. Phys. Chem. A* **111** (2007) 4456.
8. M.J. DeWitt and R.J. Levis, *J. Chem. Phys.* **102** (1995) 8670, *ibid. J. Chem. Phys.* **108** (1998) 7045, *ibid. J. Chem. Phys.* **110** (1999) 11368.
9. H.W. Jochims, E. Rühl, H. Baumgärtel, S. Tobita, and S. Leach, *Int. Jour. Mass Spec. and Ion Proc.* **167/168** (1997) 35.
10. H.W. Jochims, H. Baumgärtel, and S. Leach, *Astron. and Astrophys. J.* **314** (1996) 1003.
11. H.W. Jochims, H. Rasekh, E. Ruhl, H. Baumgärtel, S. Leach, *Chem. Phys* **168** (1992) 159.
12. E. Mejia Ospino, I. Álvarez, and C. Cisneros, *Rev. Mex. Fís.* **50** (2004) 170.
13. M.R.C. Cockett, H. Ozeki, K. Okuyama, and K. Kimura, *J. Chem. Phys.* **98** (1998) 7763.
14. J.W. McConkey, S. Trajmar, K.F. Man, and J.M. Ratliff, *J. Phys. B: At. Mol. Opt. Phys.* **25** (1992) 2197.
15. H. Spooner, C.D. Cooper, *J. Phys. Chem.* **23** (1955) 646.
16. Y. Fujimura, M. Onda, and T. Nakajima, *Bull. Chem. Soc. Japan* **46** (1973) 2034.
17. R. Pariser, *J. Chem. Phys.* **24** (1956) 250.
18. F. Salama and L.J. Allamandola, *J. Chem. Phys.* **94** (1991) 6964.
19. N.-T. Van-Oanh, P. Désesquelles, S. Douin, and Ph. Bréchnignac, *J. Phys. Chem. A* **110** (2006) 5592; *ibid.* **110** (2006) 5599.
20. F. Jobilois, A. Klotz, F.X. Gadéa, and C. Joblin, *Astronomy & Astrophysics* **444** (2005) 629.
21. Y.-P. Ho, R.C. Dumbbar, Ch. Lifshitz, *J. Am. Chem. Soc.* **117** (1995) 6504.
22. D.R. Reed, and S.R. Kass, *J. Mass Spectrometry* **35** (2000) 534.
23. Y. Gotkins, M. Oleinikova, M. Naor, and Ch. Lifshitz, *J. Phys. Chem.* **97** (1993) 12282.
24. H.W. Jochims, H. Rasejh, E. Rühl, H. Baumgärtel, and S. Leach *J. Phys. Chem.* **97** (1993) 1312.
25. S.P. Ekern, A.G. Marshall, J. Szczepanski, and M. Vala, *J. Phys. Chem. A* **102**(1998) 3498.